Journal of Soils and Sediments (2024) 24:1969–1987
https://doi.org/10.1007/s11368-024-03759-0

SOILS, SEC 3 • REMEDIATION AND MANAGEMENT OF CONTAMINATED OR DEGRADED LANDS • RESEARCH ARTICLE

# Magnetic enhancement of road dusts in Shanghai and its implications for the urban environment

Yan-Shuo Zhang[1] · Xue-Feng Hu[1] · Xin-Dong Wang[1] · Le-San Mei[1] · Yu-Ting Jia[1]

Received: 11 October 2023 / Accepted: 21 February 2024 / Published online: 6 March 2024


## Abstract

**Purpose** Road dust samples in Baoshan District, Shanghai, were collected to explore magnetic and chemical properties of atmospheric dustfall in urban areas, intensively impacted by anthropogenic activities. Magnetic particles in road dusts were separated and analyzed to track their sources and then to discuss the influences of industrial and traffic emissions on the urban environment.

**Materials and methods** One hundred twenty-two road dust samples in the industrial, traffic, residential, and agricultural areas of Baoshan District, Shanghai, were collected. Magnetic susceptibility ($\chi_{lf}$) and heavy metal content of the samples were determined. Micromorphological and microchemical features of magnetic particles separated from the road dusts were analyzed by a scanning electron microscope (SEM) equipped with energy spectrum.

**Results and discussion** The road dusts are usually alkaline and strong in magnetic signal, of which, magnetic susceptibility ($\chi_{lf}$), $838.7\times10^{-8}$ $m^3$ $kg^{-1}$ on average, is much higher than the nearby topsoils. Moreover, $\chi_{lf}$ of the industrial and traffic road dusts, $1363.0\times10^{-8}$ $m^3$ $kg^{-1}$ and $775.9\times10^{-8}$ $m^3$ $kg^{-1}$ on average, respectively, is significantly higher than that of the others. Magnetic spherules, mainly composed of Fe oxides, were commonly observed in the road dusts, which are mostly formed during industrial high-temperature processes. A high number of flake-like, rod-like, and other irregular-shaped magnetic particles were also found in the road dusts, which may come from metal processing or vehicular wearing. The road dusts in the study areas are heavily polluted by Cu, Zn, Pb, Cd, and Cr. The principal component analyses (PCA) indicate that $\chi_{lf}$ and Zn, Mn, and Fe contents in the road dusts belong to the same principal component.

**Conclusions** Magnetic dustfall commonly occurs in urban areas due to industrial or vehicular emissions, which leads to the enhancement of magnetic signal and heavy metal content in urban road dusts simultaneously. $\chi_{lf}$ can indicate the accumulation of toxic heavy metals in the road dusts effectively. This also highlights a fact that the urban environment is continuously and significantly affected by the deposition of artificial atmospheric magnetic particles.

**Keywords** Road dusts · Magnetic susceptibility ($\chi_{lf}$) · Heavy metals · Industrial emissions

## 1 Introduction

Road dust is mainly formed by the dry or wet depositions of atmospheric suspended particles, which, however, often varies in origin (Gunawardana et al. 2012; Liu et al. 2014). Natural dust on roads stems from the deposition of loessic materials, which are transported from remote sources, or re-deposition of raised local soil. Under the urban environment, the materials of road dust are highly influenced by industrial and traffic emissions, which mostly come from the settlements of fly ashes emitted from industrial or petrochemical fuel combustion, or particles produced by vehicular exhausts or frictions (Abbasi et al. 2020; Logiewa et al. 2020; Pant and Harrison 2013; Petrovský et al. 2013; Wei and Yang 2010; Yang et al. 2010). A high amount of fine black particles are emitted by iron processing industries, causing metal dust (Kacer et al. 2023). The road dust with dense traffic often contains higher content

Responsible editor: Claudio Colombo

✉ Xue-Feng Hu
xfhu@shu.edu.cn

[1] School of Environmental and Chemical Engineering, Shanghai University, Shanghai 200444, People's Republic of China

of metal particles produced by frictions of vehicular brakes, while that in rural areas is mostly composed of soils (Panko et al. 2013).

Highly affected by industrial and traffic emissions, atmospheric suspended particles in urban areas often contain a certain amount of metal dust, especially ferromagnetic particles combined with toxic heavy metals. The deposition of magnetic dusts makes magnetic signal and heavy metal content of urban topsoils enhanced simultaneously (Fabijańczyk et al. 2016; Liu et al. 2016; Yang et al. 2007), thus highly changing the properties of urban soils (Li and Feng 2010; Magiera et al. 2018). Moreover, significant correlations between magnetic parameters and heavy metal contents in urban soils were reported worldwide (Cao et al. 2015; Jordanova et al. 2013; Karimi et al. 2011; Xia et al. 2014; Yang et al. 2020). The soils closer to the iron smelting complex are much higher in magnetic susceptibility ($\chi_{lf}$) in Baoshan District of Shanghai (Hu et al. 2022, 2007). Magnetic spherules were observed in urban soils (Lu et al. 2016; Wang et al. 2017), further proving the deposition of anthropogenic magnetic particles on the urban ground.

The constituents of urban soils, however, are much complicated. Especially, magnetic particles accumulated in urban soils are often multiple in provenances, which may be inherited from parent rocks, produced by pedogenic processes, or stem from anthropogenic activities. On the contrary, the dust on urban solidified roads solely comes from the deposition of atmospheric particles due to routine road cleaning. Therefore, it can reflect atmospheric quality and metallic or magnetic deposition under the urban environment more directly (Ali et al. 2017; Bucko et al. 2011; Dytłow et al. 2019; Górka-Kostrubiec et al. 2023).

Fe-rich magnetic spherules are observed in road dust (Bourliva et al. 2016), which mainly comes from industrial high-temperature combustion (Jordanova et al. 2021) or coal burning (Jose and Srimuruganandam 2021). Located in the northern part of Shanghai, Baoshan District is an important metallurgical industrial base in China. The accumulation of toxic heavy metals and magnetic particles in the soils of the district has been intensively studied over the past decades (Hu et al. 2022, 2007; Ye et al. 2007). Road dust in the district, which may indicate the influences of anthropogenic emissions on the urban environment more clearly and directly, is still less studied however.

In this study, 122 dust samples on the solidified roads at four different land use surface in the district are collected. We aim to measure the magnetic signal of the road dust to scrutinize whether it is also enhanced like that of topsoil in the district, then to track the sources of magnetic particles accumulated in it, further to study the correlations between magnetic signal and heavy metal in the road dust, and finally to discuss the implications of magnetic enhancement in the road dust on the urban environment.

## 2 Materials and methods

### 2.1 Study area

Located at the frontier of the Yangtze River Delta, Shanghai is close to the East China Sea on the east, with geographic location of 30°40′N~31°53′N and 120°51′E~122°12′E. Shanghai has a subtropical monsoonal climate, with mean annual temperature16.6 ℃ and mean annual precipitation 1168.1 mm. Baoshan District is situated in the northern part of Shanghai, adjoining the Yangtze River Estuary in the northeast (Fig. 1). It covers 365.3 $km^2$ in area, including Luojing, Yuepu, Luodian, Yanghang, Gucun, Songnan, and Dachang Towns, with a permanent population of 2,235,000. As a traditional industrial base of Shanghai, Baoshan District has developed a huge industrial system dominated by ironic smelting and processing, where shipping, railways, highways, urban roads and inland waterways are interconnected, forming a large and developed network of transportation.

### 2.2 Sample collection

According to different land use surface, four functional areas, namely, industrial, traffic, residential, and agricultural areas, were circled in Baoshan District, Shanghai. More sampling points were arranged in the industrial and traffic areas, as more intensively impacted by anthropogenic activities. After seven consecutive sunny days from Sep 2022 to Dec 2022, 37, 40, 23, and 22 dust samples were collected on the solidified road surface of the four areas, using clean brushes, respectively (Fig. 1). One sample, about 150 g in weight, was a mixture of three subsamples, all collected within a range of 20×20 $m^2$ at a sampling point. The samples were carried to the laboratory, air-dried, and passed through 2-mm nylon sieve to discard weeds, gravel, leaves, and other debris. It was then passed through 0.149-mm nylon sieve. The dominant fraction (<0.149 mm) of the samples was mainly used for physical and chemical analyses.

### 2.3 Determination of pH and organic matter content

Dust sample of 4.00 g (<0.149 mm) was added with 10 ml deionized water and stirred. The electrode of a pH meter was put into the dust-water suspension for measuring pH value. About 1 g sample (<0.149 mm) was weighed to determine the content of organic matter by the $K_2CrO_7$-$H_2SO_4$ method (USDA and NRCS 2004; Zhang and Gong 2012).

### 2.4 Magnetic measurements

Road dust sample of 5.00 g (<0.149 mm) was weighed and wrapped using plastic film and fixed into a 10-ml cylindrical polyethylene box. The sample boxes were then put into

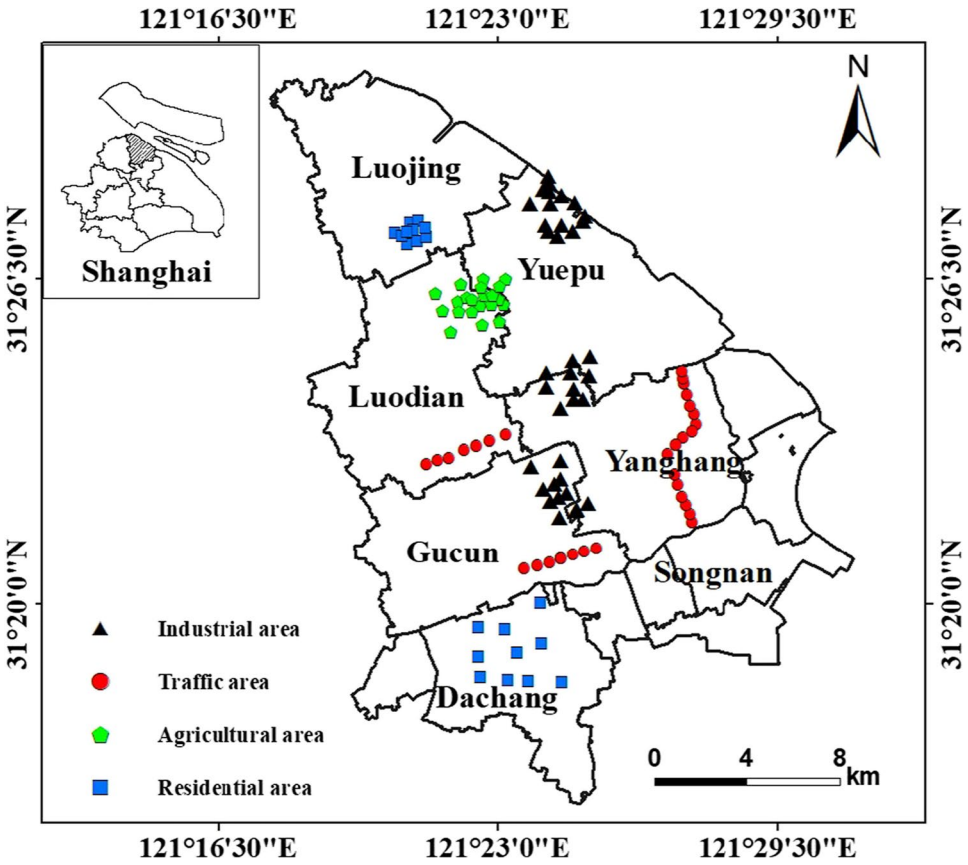


**Fig. 1** Sketch map showing the points of sampling road dust in the industrial, traffic, agricultural, and residential areas of Baoshan District, northern Shanghai, Southeast China. A shadow square in the inset map on the upper left corner shows the location of the study areas in Shanghai

a Bartington MS-2 magnetic susceptibility meter to measure the magnetic susceptibility in low frequency (0.47 kHz) ($\chi_{lf}$) and high frequency (4.7 kHz) ($\chi_{hf}$). Each sample was measured for three times, and the relative error was < 0.3%. The frequency susceptibility ($\chi_{fd}$%) was calculated by the following formula:

$$\chi_{fd}\% = (\chi_{lf} - \chi_{hf})/\chi_{lf} \times 100\%$$

## 2.5 Determination of heavy metal content

About 0.2 g road dust sample (< 0.149 mm) was put into a Teflon crucible and digested using three mixed acids ($HNO_3 + HF + HClO_4$). The concentrations of Cu, Zn, Cr, Co, Ni, Mn, and Fe in the digested solutions were determined using an inductively coupled plasma atomic emission spectrometer (ICP-AES) (Leeman Prodigy ICP AES, USA); Pb and Cd were determined using a graphite furnace atomic absorption spectrometer (GF-AAS) (ZEEnit600/650, Jena, Germany). During the testing processes, some samples randomly selected were repeatedly measured for five times, in which, the relative standard deviations of the contents of heavy metal were mostly ≤ 3.58%, and Co was ≤ 5.92%. A standard soil sample, GSS-5, produced by China Environmental Monitoring Station, was inserted during the testing. The relative error between the measured and reference values of heavy metals in the standard was mostly ≤ 2.95%, and Co was ≤ 9.25%.

## 2.6 Separation of magnetic fraction from road dust samples

Road dust sample of 100 g (< 2 mm) was put into a beaker and added with 0.05 mol $L^{-1}$sodium hexametaphosphate solution. The muddy solution was continuously stirred and then maintained overnight. A strong magnet wrapped with plastic film was slowly rotated in the beaker to fully adsorb magnetic particles in the solution. The wrapped magnet was removed from the solution and washed with deionized water to get rid of muddy impurities. The plastic film was then separated from the magnet, and magnetic particles on the film were immediately washed into another clean beaker with deionized water. Such operation was repeated for several times until few magnetic particles were extracted from the solution. The extracted magnetic materials were washed into a tube, centrifuged, and then dried at 50 ℃ in oven to get a purified magnetic fraction.

### 2.7 Micromorphological analyses of single magnetic particles

Single magnetic particles were chosen from the separated magnetic fractions using a microscope and were gold-plated in a vacuum container using Au ion sputtering method. The prepared gold-plated particles were put into the ZEISS Gemini 300 scanning electron microscope (SEM) to observe the microscopic morphology of magnetic particles. The chemical composition of a selected position of a magnetic particle was enlarged, scanned, and finally semi-quantitatively analyzed by the energy spectrum analysis affiliated to the SEM.

### 2.8 Calculation of pollution indexes

Single-factor Pollution Index (SPI) and Pollution Load Index (PLI) are used to assess the degree of heavy metal pollution of road dusts. SPI was calculated as the formula:

$$CFi = Ci/C0.$$

Here, $CF_i$ is the SPI of heavy metal $i$; $C_i$ is the measured concentration of heavy metal $i$ in the road dusts; and $C_0$ is the background value of heavy metal $i$ in the soils of Shanghai (Hu et al. 2007).

PLI reflecting a comprehensive pollution degree of an area was calculated as $(CF_1 \times CF_2 \times CF_3 \times \ldots \times CF_n)^{1/n}$, of which, $n$ is the number of heavy metals participating in the assessment.

Based on the values of SPI or PLI, four levels of pollution are classified, including non-pollution ($\leq 1.0$), slight pollution ($>1.0$ and $\leq 2.0$), moderate pollution ($>2.0$ and $\leq 3.0$), and heavy pollution ($>3.0$) (Tomlinson et al. 1980).

### 2.9 Data treatments

All the data were firstly processed by Microsoft Excel 2016.The sketch map of the study areas was drawn using ArcGIS Map10.8.1. Statistical analyses, including analysis of variance (one-way ANOVA), Pearson correlations, and principal component analysis (PCA) were performed by IBM SPSS Statistics 24. The box diagrams were drawn using Origin 2018.

## 3 Results

### 3.1 pH and organic matter content of road dusts

The road dusts are mostly alkaline, of which, pH is in a range of 7.2–10.9 (Table 1). Moreover, pH of the road dusts on the different functional areas varies highly. That on the industrial, agricultural, traffic, and residential areas is 9.3, 8.3, 8.2, and 7.8 on average, respectively (Fig. 2a). pH of the industrial road dust (the road dust on the industrial area; the same below) is significantly higher than that of the others ($p<0.05$) (Fig. 2a), hinting the addition of alkaline materials due to industrial emissions.

The content of organic matter in the road dusts of the study areas is 71.5 g $kg^{-1}$ on average. That on the industrial, residential, traffic, and agricultural areas is 90.3, 84.0, 61.2, and 41.6 g $kg^{-1}$ on average, respectively (Fig. 2b). Organic matter content on the industrial and residential road dusts is significantly higher than that on the traffic and agricultural ($p<0.05$) (Fig. 2b). This suggests that a higher amount of organic pollutants were emitted from industrial and dweller daily life.

**Table 1** Magnetic susceptibility ($\chi_{lf}$) and physical-chemical properties of road dusts in the different functional areas of Baoshan District in Shanghai, Southeast China

| Functional areas | Items | pH | Organic matter (g $kg^{-1}$) | $\chi_{lf}$ ($\times 10^{-8} m^3 kg^{-1}$) | $\chi_{fd}$ (%) |
|---|---|---|---|---|---|
| Industrial ($n=40$) | Maximum | 10.9 | 253.6 | 3367.3 | 4.53 |
| | Minimum | 7.7 | 20.2 | 436.0 | 0.0 |
| | Mean | 9.3 | 90.3 | 1363.0 | 0.76 |
| | CV (%) | 8.9 | 56.1 | 44.8 | 79.6 |
| Traffic ($n=37$) | Maximum | 8.9 | 111.3 | 1482.0 | 2.62 |
| | Minimum | 7.3 | 46.4 | 448.0 | 0.0 |
| | Mean | 8.2 | 61.2 | 775.9 | 0.73 |
| | CV (%) | 3.6 | 25.1 | 33.2 | 87.7 |
| Residential ($n=23$) | Maximum | 8.4 | 156.9 | 771.3 | 3.51 |
| | Minimum | 7.2 | 44.3 | 106.0 | 0.21 |
| | Mean | 7.8 | 84.0 | 357.2 | 1.38 |
| | CV (%) | 2.2 | 17.5 | 20.0 | 63.4 |
| Agricultural ($n=22$) | Maximum | 8.9 | 56.8 | 910 | 2.66 |
| | Minimum | 8.0 | 28.1 | 174.0 | 0.0 |
| | Mean | 8.3 | 41.6 | 494.3 | 0.95 |
| | CV (%) | 2.9 | 17.4 | 60.7 | 64.2 |

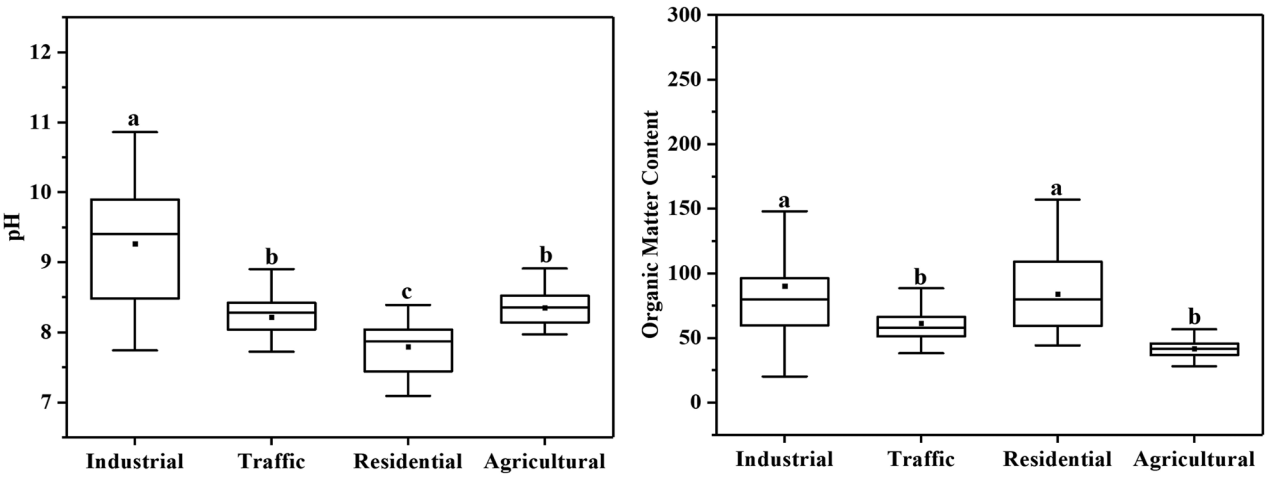


**Fig. 2** Variation of pH (Left) and organic matter content (Right) of the road dusts in the different functional areas of Baoshan District, Shanghai, Southeast China

### 3.2 $\chi_{lf}$ of road dusts

$X_{lf}$ values of the road dusts on the study areas are in a range of 175.3 to $3367.3\times10^{-8}$ $m^3$ $kg^{-1}$, with a mean of $838.7\times10^{-8}$ $m^3$ $kg^{-1}$, about 29 times the magnetic background of the soils in Shanghai (Hu et al. 2007). Likewise, $\chi_{lf}$ of the road dusts in the different functional areas is highly different (Table 1).

$\chi_{lf}$ of the industrial road dusts is $1363.0\times10^{-8}$ $m^3$ $kg^{-1}$ on average, with the coefficient of variation (CV) being 44.8%. A maximum occurs at Site No. 36 nearby some machinery and metal processing plants, reaching as high as $3367.3\times10^{-8}$ $m^3$ $kg^{-1}$, 115.6 times the magnetic background of the soils in Shanghai (Hu et al. 2007). That at Site Nos. 35, 37, and 41 nearby concrete and steel plants is more than $2038\times10^{-8}$ $m^3$ $kg^{-1}$, 70 times the magnetic background.

$\chi_{lf}$ of the traffic road dusts is $775.9\times10^{-8}$ $m^3$ $kg^{-1}$ on average, with the CV being 33.2%. That at Site Nos. 1 and 12 located at the junction between the outer-ring express way and the Hui-Tai Highway is higher than $1164.7\times10^{-8}$ $m^3$ $kg^{-1}$, 40 times the magnetic background. The junction has witnessed an extremely busy traffic.

$\chi_{lf}$ of the residential areas is $357.2\times10^{-8}$ $m^3$ $kg^{-1}$ on average, with the CV being 20.0%. The samples of the agricultural road dusts are mostly collected on solidified road surfaces near vegetable greenhouses and fields, of which, $\chi_{lf}$ is $494.3\times10^{-8}$ $m^3$ $kg^{-1}$ on average, with the CV being 60.7%. Only that at Site No. 63 nearby the intersection of two traffic lines is anomalously high, $910\times10^{-8}$ $m^3$ $kg^{-1}$.

$\chi_{fd}$% can roughly indicate the concentration of Superfine paramagnetic particles (SP) in soils or sediments. It is believed to contain few SP when $\chi_{fd}$% is < 2% (Dearing et al. 1996). In this study, $\chi_{fd}$% of the industrial, traffic, residential, and agricultural road dusts are 0.79%, 0.73%, 1.47%, and 0.98% on average, respectively.

### 3.3 Micromorphological features of magnetic particles separated from road dusts

A high amount of magnetic spherules were observed in the magnetic fractions separated from the road dusts, mostly in a range of 10–100 μm in grain size (Fig. 4). The spherules in the industrial road dusts are more and coarser, ranging from 20 to 100 μm; those in the traffic range from 10 to 80 μm in grain size; and those in the residential and agricultural are less and finer, ranging from 10 to 50 μm in grain size.

Moreover, the magnetic spherules highly vary in morphological features, mainly including five surface types, namely, round, hollow, coral reef-like, encephalon-like, and mother-son ball surfaces (Fig. 5). The chemical composition of the spherules, however, is much similar, including Fe (62.23~74.61%), O (20.81~29.05%), and other elements of C, Al, Ca, and Si as impurities (Fig. 6).

There are also many non-spherical magnetic particles separated from the road dusts, showing brick-like, flake-like, prismatic, rod-like, stalactite-like, and polymeric forms (Figs. 5 and 7). Like magnetic spherules, most non-spherical particles are also dominantly composed of Fe (Fig. 7a). Some are mainly composed of Fe, O, Zn, and Cr (Fig. 7b); some composed of Fe, Si, Al, and Ca (Fig. 7c); and some composed of O, Zn, C, Ti, and Fe (Fig. 7d).

### 3.4 Heavy metal accumulation in road dusts

The contents of Cu, Zn, Pb, Cd, Cr, Co, Ni, Mn, and Fe in the road dusts of the study areas are 94.1, 368.6, 204.3, 0.622, 282.0, 13.6, 45.9, and 901.3 mg $kg^{-1}$ and 53.1 g $kg^{-1}$ on average, respectively (Table 2). Cu, Zn, Pb, Cd, and Cr contents in the road dusts are significantly higher than the background values of the soils in Shanghai (Wang et al.

**Table 2** Contents of heavy metals in the road dusts in Baoshan District, Shanghai, Southeast China

| District | Items | Cu (mg $kg^{-1}$) | Zn (mg $kg^{-1}$) | Pb (mg $kg^{-1}$) | Cd (mg $kg^{-1}$) | Cr (mg $kg^{-1}$) | Co (mg $kg^{-1}$) | Ni (mg $kg^{-1}$) | Mn (mg $kg^{-1}$) | Fe (g $kg^{-1}$) |
|---|---|---|---|---|---|---|---|---|---|---|
| Industrial area ($n=40$) | Maximum | 199.1 | 1596.8 | 312.5 | 1.121 | 749.2 | 54.9 | 123.9 | 2090.1 | 189.7 |
| | Minimum | 28.5 | 131.9 | 38.0 | 0.240 | 106.5 | 3.2 | 12.4 | 577.7 | 36.0 |
| | Mean | 77.1 | 522.2 | 113.0 | 0.588 | 277.1 | 14.6 | 52.4 | 1151.2 | 79.1 |
| | CV (%) | 54.4 | 59.8 | 46.4 | 33.7 | 51.9 | 71.5 | 53.9 | 35.4 | 41.1 |
| Traffic area ($n=37$) | Maximum | 349.4 | 773.8 | 632.7 | 1.434 | 1453.1 | 37.9 | 97.6 | 1709.81 | 92.3 |
| | Minimum | 52.5 | 71.0 | 30.6 | 0.288 | 120.4 | 5.3 | 17.5 | 296.4 | 14.2 |
| | Mean | 139.0 | 309.2 | 188.6 | 0.648 | 389.7 | 17.2 | 44.9 | 831.9 | 49.7 |
| | CV (%) | 54.2 | 48.1 | 54.9 | 38.8 | 66.2 | 49.5 | 38.0 | 38.1 | 31.7 |
| Residential area ($n=23$) | Maximum | 201.2 | 606.5 | 4131.4 | 2.699 | 344.4 | 13.1 | 81.1 | 1002.7 | 52.6 |
| | Minimum | 28.1 | 114.0 | 79.6 | 0.280 | 75.7 | 5.4 | 17.5 | 389.3 | 6.8 |
| | Mean | 68.9 | 270.5 | 428.8 | 0.739 | 168.0 | 9.0 | 36.4 | 632.0 | 30.9 |
| | CV (%) | 26.7 | 25.8 | 95.8 | 37.3 | 18.7 | 11.0 | 23.4 | 12.1 | 15.7 |
| Agricultural area ($n=22$) | Maximum | 147.2 | 418.0 | 256.8 | 0.682 | 448.4 | 23.5 | 87.9 | 1546.6 | 60.6 |
| | Minimum | 31.0 | 71.0 | 40.2 | 0.280 | 94.6 | 5.4 | 20.8 | 527.3 | 6.1 |
| | Mean | 75.8 | 291.8 | 162.2 | 0.521 | 229.0 | 10.8 | 45.6 | 844.9 | 34.8 |
| | CV (%) | 37.0 | 20.6 | 32.3 | 21.0 | 39.4 | 46.8 | 45.2 | 30.5 | 58.1 |
| Average dust value | | 94.1 | 368.6 | 204.3 | 0.622 | 282.0 | 13.6 | 45.9 | 901.3 | 53.1 |
| Shanghai soil background value (Wang et al. 1992) | | 28.6 | 86.1 | 25.5 | 0.13 | 75.0 | 12.7 | 31.9 | 560.2 | 30.2 |

1992). Especially, Zn, Cd, and Pb contents in the road dusts are 4.3, 4.8, and 8.0 times the soil background values, respectively.

The contents of heavy metals in the road dusts of the study areas also vary from site to site, with the CVs of Pb, Cr, Cu, Zn, Co, Fe, Cd, Ni, and Mn being 186.08%, 66.99%, 63.61%, 63.45%, 62.46%, 56.24%, 49.90%, 49.33%, and 41.12%, respectively (Table 2). These in the different functional areas are highly different. Zn, Mn, and Fe contents in the industrial road dusts are significantly higher than those in the residential and agricultural ($p<0.05$) (Table 3). Cu, Cr, and Co in the traffic road dusts are significantly higher than those in the residential and agricultural ($p<0.05$). Notably, Cr content in the traffic road dusts is even higher than that in the industrial. Cr content at Site No. 12 located beside the outer-ring of expressway is as high as 1453.1 mg $kg^{-1}$, 19.4 times the soil background value. Anomaly of Pb content in the residential road dusts was also observed. Pb content at Site No. 61 in the residential areas, for example, reaches as high as 4131.4 mg $kg^{-1}$, 162 times the soil background value.

## 4 Discussion

### 4.1 Magnetic enhancement of urban road dusts

The dust accumulated on solidified road surface is mostly formed by dry and wet depositions of atmospheric suspended particulate matter. Compared with soil, it reflects local atmospheric quality more directly. Natural dustfall varies from 80 to $150\times10^{-8}$ $m^3$ $kg^{-1}$ in $\chi_{lf}$ in the Loess Plateau, Northwest China (Sun et al. 2001). Modern loess in Lantian in the northern part of the Loess Plateau, Northwest China, is about $53\times10^{-8}$ $m^3$ $kg^{-1}$ in $\chi_{lf}$ on average (Rao et al. 2015). This means that natural dustfall far away from urban areas is not so high in magnetic background. In contrast, the dustfall and road dust in metropolises are often extremely strong in magnetic signal. As far as we know, $\chi_{lf}$ of the road dust in West Midlands, UK, is $588.3\times10^{-8}$ $m^3$ $kg^{-1}$ on average (Shilton et al. 2005); that in Asaluye, Iran, is $550.9\times10^{-8}$ $m^3$ $kg^{-1}$ (Abbasi et al. 2020); that in Lanzhou City, Northwest China, is $442.4\times10^{-8}$ $m^3$ $kg^{-1}$ (Wang et al. 2012); that in Thessaloniki, Greece, is $408.7\times10^{-8}$ $m^3$ $kg^{-1}$ (Bourliva et al. 2018); and that in Sofia, Bulgaria, is $264.6\times10^{-8}$ $m^3$ $kg^{-1}$ (Jordanova et al. 2014).

Generally, $\chi_{lf}$ of the road dusts in Baoshan District, Shanghai, $838.7\times10^{-8}$ $m^3$ $kg^{-1}$ on average, is much higher than that in the other cities worldwide (Fig. 3). Moreover, the road dusts vary in magnetic signal in the different functional areas. The industrial and traffic road dusts are even more significantly enhanced (Fig. 3). $\chi_{lf}$ of the industrial road dust, $1363.0\times10^{-8}$ $m^3$ $kg^{-1}$ on average, is significantly higher than that of the others, while $\chi_{lf}$ of the traffic road dust ($p<0.05$), $775.9\times10^{-8}$ $m^3$ $kg^{-1}$ on average, is significantly higher than that of the

**Table 3** Contents of heavy metals in the road dusts in the different functional areas in Baoshan District, Shanghai, Southeast China

| Functional areas | $\chi_{lf}$ ($\times10^{-8}$ $m^3$ $kg^{-1}$) | Cu (mg $kg^{-1}$) | Zn (mg $kg^{-1}$) | Pb (mg $kg^{-1}$) | Cd (mg $kg^{-1}$) | Cr (mg $kg^{-1}$) | Co (mg $kg^{-1}$) | Ni (mg $kg^{-1}$) | Mn (mg $kg^{-1}$) | Fe (g $kg^{-1}$) |
|---|---|---|---|---|---|---|---|---|---|---|
| Industrial | 1363.0 ± 617.8a | 77.1.0 ± 42.5b | 522.2 ± 316.4a | 113.0 ± 53.1b | 0.59 ± 0.20ab | 277.1 ± 145.8b | 14.6 ± 10.6ab | 52.4 ± 28.6a | 1151.2 ± 412.2a | 79.1 ± 32.9a |
| Traffic | 775.9 ± 261.1b | 139.0 ± 76.4a | 309.2 ± 150.2b | 188.6 ± 105.0b | 0.65 ± 0.25ab | 389.7 ± 261.7a | 17.2 ± 8.60a | 44.9 ± 17.3ab | 831.9 ± 321.5b | 49.7 ± 16.0b |
| Residential | 357.2 ± 146.0c | 68.9 ± 37.6b | 270.5 ± 142.7b | 428.8 ± 840.2a | 0.74 ± 0.56a | 168.0 ± 64.2b | 9.03 ± 2.03c | 36.4 ± 17.4b | 632.0 ± 155.9b | 30.9 ± 9.9c |
| Agricultural | 494.3 ± 307.3c | 75.8 ± 28.7b | 291.8 ± 61.6b | 162.2 ± 53.7b | 0.52 ± 0.11b | 229.0 ± 92.4b | 10.8 ± 5.16bc | 45.6 ± 21.1ab | 844.9 ± 263.9b | 34.8 ± 20.7bc |

Data in the table are expressed as mean ± standard deviation (SD); the data in the same column marked with different lowercase letters indicate significant difference ($p<0.05$)

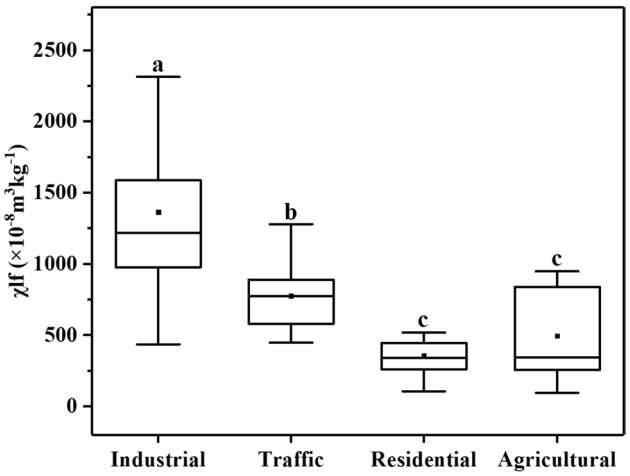


**Fig. 3** Variation of magnetic susceptibility ($\chi_{lf}$) of the road dusts in the different functional areas of Baoshan District, Shanghai, Southeast China

residential and agricultural road dusts ($p < 0.05$) (Fig. 3). In addition, the industrial road dust is more alkaline and are significantly higher in pH and organic matter content than the others ($p < 0.05$) (Fig. 2). This highly suggests that the accumulation of magnetic substances in the road dusts of the study areas is mainly attributed to the deposition of alkaline Fe-bearing dustfall emitted from industries and vehicles.

SP in soil are dominantly produced during the pedogenic weathering processes, while multi-domain (MD) and stable single-domain (SSD) grains are mainly formed from anthropogenic activities. All of the road dust samples of the study areas have $\chi_{fd}$% less than 4%, while 89.3% have $\chi_{fd}$% less than 2%. The industrial and traffic road dusts are only 0.76% and 0.73%in $\chi_{fd}$% on average, respectively. It fully suggests that the road dusts in Baoshan District are dominantly enriched in coarse magnetic particles, originating from industrial and vehicular emissions. The accumulation of magnetic substances in the road dusts highlights a fact of the continuous settlement of anthropogenic magnetic particles in the urban environment.

## 4.2 Tracking the sources of magnetic particles in urban road dusts

Magnetic spherules, 5–150 μm in grain size, were previously observed in urban topsoils and atmospheric suspended particles in Baoshan District, Shanghai (Hu et al. 2022). In this study, a high number of similar magnetic spherules were also found in the road dusts (Fig. 4). The spherules are mostly produced during high-temperature combustion, which are commonly seen in the urban soil and environment around smelting industries and coal-fired power plants (Wang et al. 2019). It was also found in automobile exhausts (Aguilar et al. 2021). Fe-rich spherules are usually released during industrial smelting and ore (coal) combustion as a round shape is the lowest in energy when high-temperature molten iron or ore are condensed.

In this study, magnetic spherules observed in the industrial and traffic road dusts are more in content r and coarser in grain size, mostly ranging from 50 to 100 μm. These in the residential and agricultural are less and finer, mostly ranging from 10 to 20 μm, as relatively far away from industrial smelting and coal-burning power plants (Fig. 4).

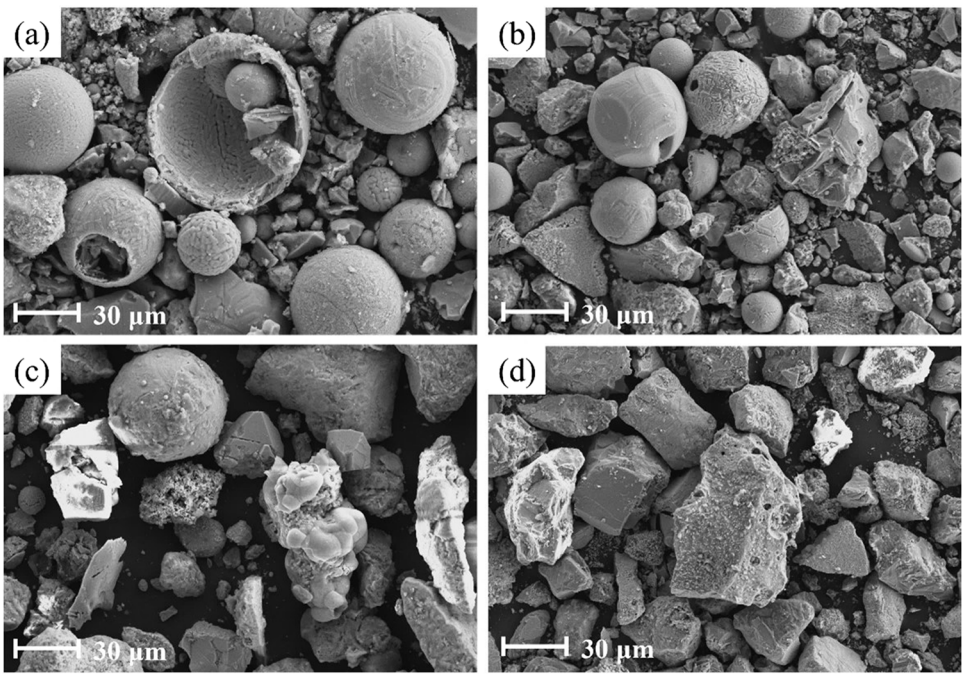


**Fig. 4** Micromorphological characteristics of magnetic particles separated from the road dusts in the industrial **a**, traffic **b**, residential **c**, and agricultural **d** areas in Baoshan District, Shanghai, Southeast China

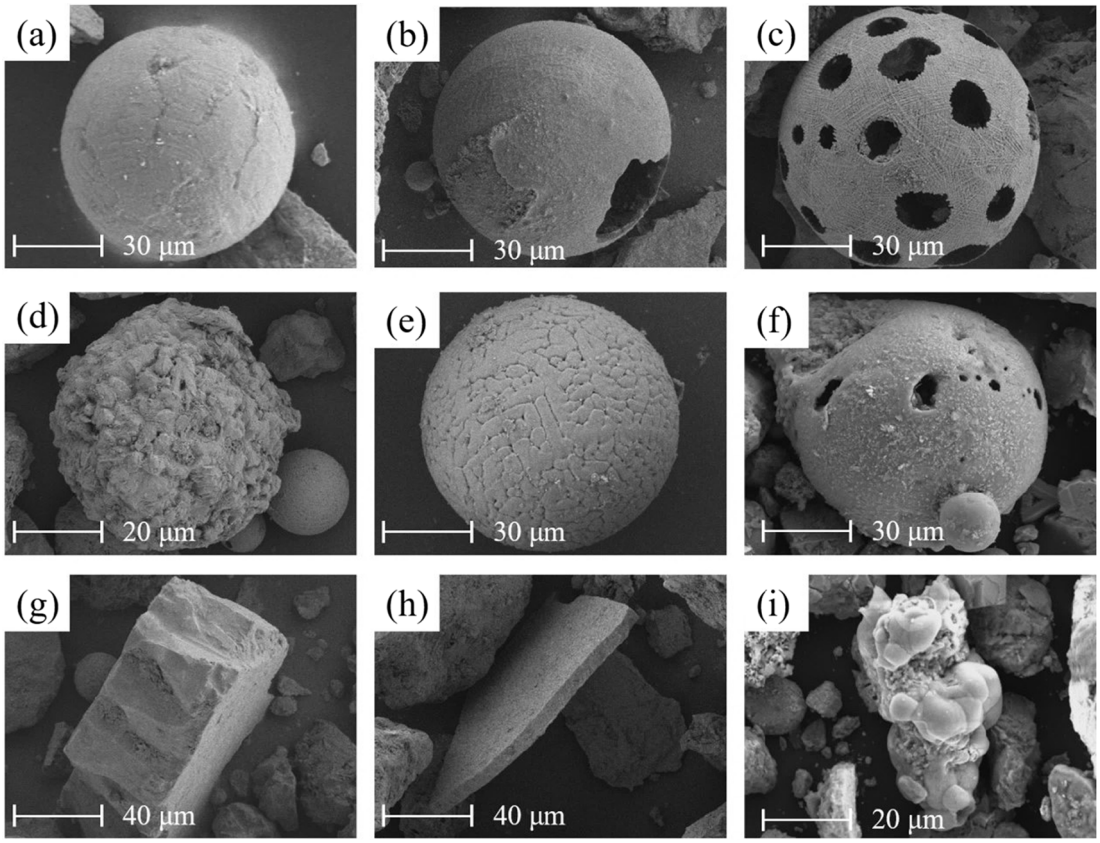


**Fig. 5** Micromorphological characteristics of magnetic spherules **a**–**f** and non-spherical particles **g**–**i** separated from the road dusts in Baoshan District, Shanghai, Southeast China. The spherules show round and smooth **a**, hollow **b** and **c**, coral reef-like **d**, and encephalon-like **e** surfaces, as well as a big ball adhered with tiny balls **f**. The non-spherical particles show brick-like **g**, flake-like **h**, and stalactite-like **i** forms

This further suggests that magnetic spherules accumulated in the road dusts mostly come from industrial and vehicular emissions.

Magnetic spherules in the road dusts vary in micromorphological features, of which, five types were identified (Figs. 5 and 7). Some spherules show smoothly round surface, some have holes in body, some have encephalon-like or reef-like surfaces, and some are adhered with smaller pellets, which are basically comparable to these separated from urban topsoils as previously reported (Gunawardana et al. 2012; Jose and Srimuruganandam 2021; Lu et al. 2016). The variation in shape and structure of spherules is mainly due to the change of forming conditions, such as temperature, chemical composition, and cooling time (Blaha et al. 2008). The spherules with hollow surface (Fig. 5b, c), for example, reflects the escape of gases during high-temperature condensation, and these with encephalon-like surface (Fig. 5e) may indicate the processes of high-temperature melting and solidification. All reflect the characteristics formed by industrial high-temperature combustion or fossil burning, consistent with many previous results (Gunawardana et al. 2012; Jose and Srimuruganandam 2021; Lu et al. 2016).

The chemical composition of magnetic spherules is much similar, in which, Fe content is between 62.23 and 74.61%, and O is between 20.81 and 29.05% (Fig. 6). According to the chemical composition, magnetic spherules can be further divided into two types. The first is dominantly composed of Fe oxides, with Fe and O accounting for about 95%; the second is also mainly composed of Fe oxides, accompanied by a small amount of Al, Mg, Ca, Si, and other elements as impurities (Fig. 6). It was found that the first type mostly appears in the industrial areas, and the second mostly occurs in the traffic area.

Magnetic spherules produced during industrial high-temperature combustion are mainly composed of Fe oxides (Magiera et al. 2011). These in fly ashes produced by power plants are also dominated by Fe oxide minerals, formed by the oxidation process of iron-bearing minerals (Strzałkowska 2022). Magnesite is the dominant mineral phase of magnetic particles in the road dust collected in Merida, Mexico (Aguilar et al. 2021). The parameters of the Mössbauer spectra indicated that anthropogenic magnetic particles in the urban topsoils are magnetite-like minerals (Magiera et al. 2021). Magnetite, nicopyrite, and other Fe oxide minerals

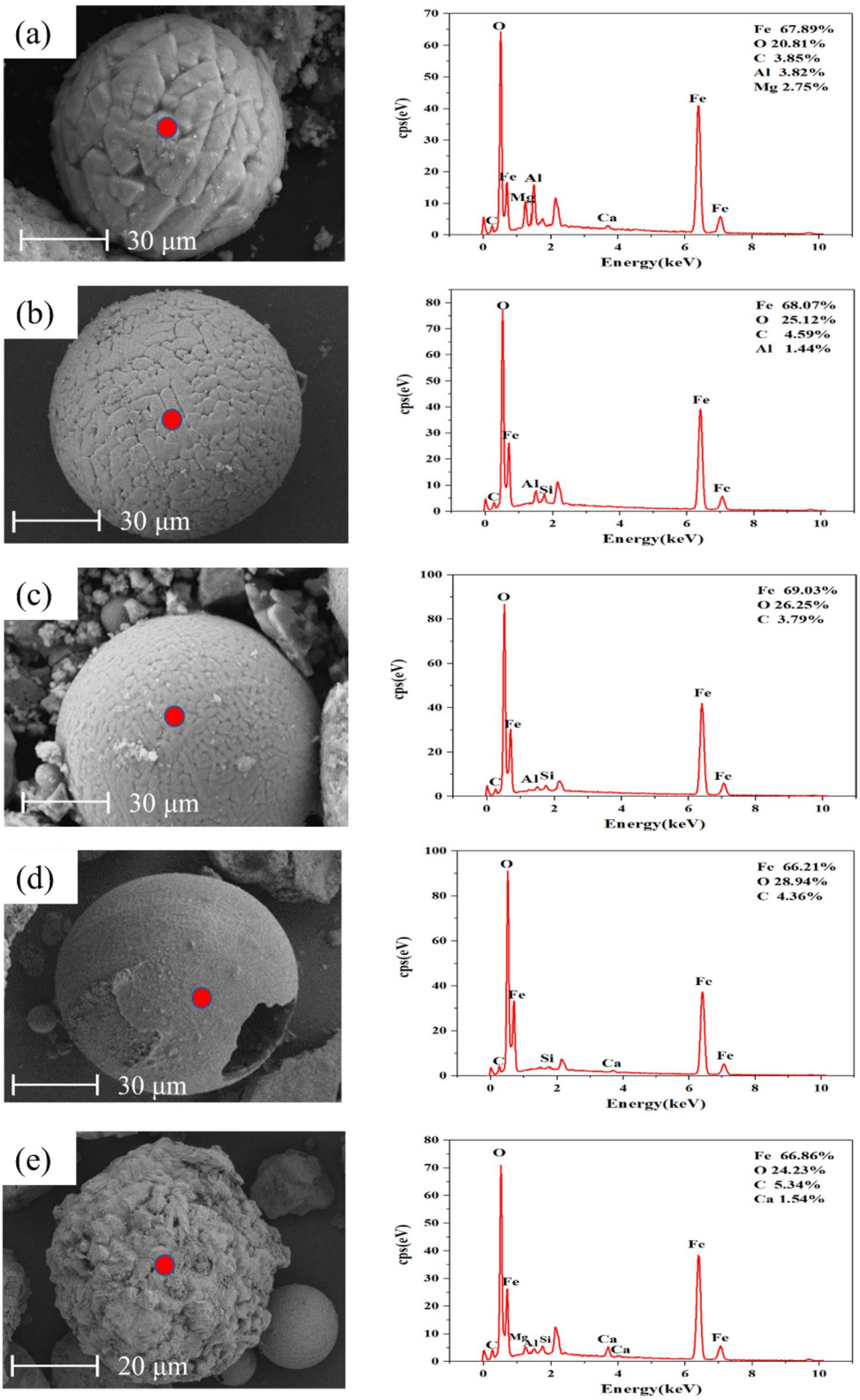


**Fig. 6** Micromorphological (left) and microchemical (right) characteristics of magnetic spherules, separated from the road dusts in Baoshan District, Shanghai, Southeast China, showing encephalon-like **a**, **b** and **c**, hollow **d**, and coral reef-like **e** surfaces, also indicating the chemical composition at the red spots of the spherules probed by the energy spectrum analysis

were identified in the magnetic fractions of urban soils in Shanghai (Hu et al. 2022).

Non-spherical magnetic particles commonly occur in urban road dust intensively impacted by industrial and traffic (Wang et al. 2019). A flake-shaped particle (Fig. 7a), mainly composed of Fe (97.32%), C (1.11%), O (0.55%), Si (0.24%), and Al (0.17%) (Fig. 7a), was found beside a machinery factory in Gucun Town, possibly emitted from the nearby iron

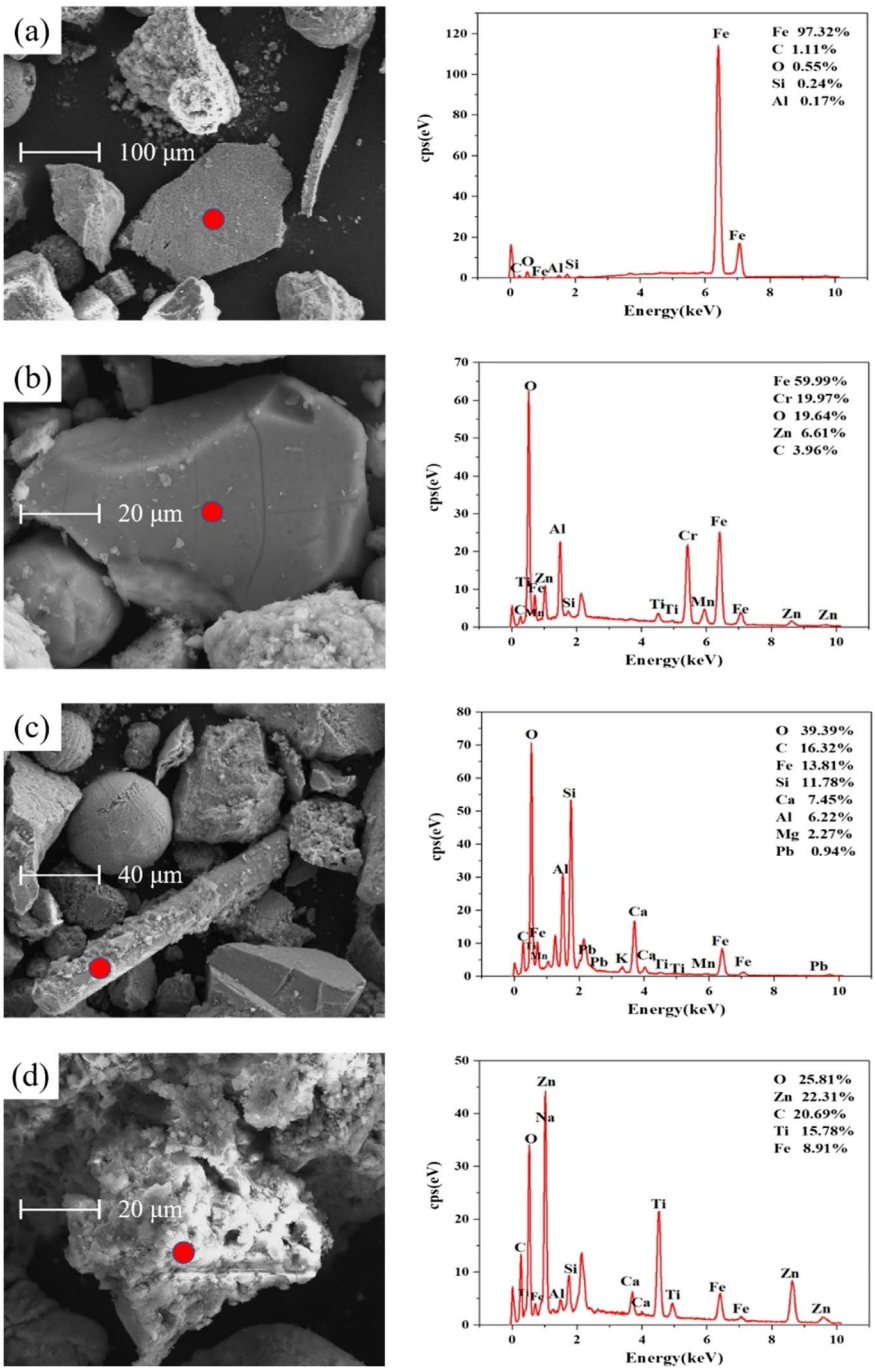


**Fig. 7** Micromorphological and microchemical characteristics of non-spherical magnetic particles separated from the urban road dusts in Baoshan District, Shanghai, Southeast China, showing flake-like **a**, prismatic **b**, rod-like **c**, and polymeric **d** forms, also indicating the chemical composition at the red spots of the particles probed by the energy spectrum analysis

processing factory. A rod-shaped magnetic particle (Fig. 7c), mainly composed of Fe, Al, Ca, Fe, Mg, C, and Si, was observed beside the outer-ring expressway, whose chemical composition and proportion are much similar to that of automotive brake pads (Table 4) and may be derived from the wearing of brake pads. This was also reported by a previous study (Kim et al. 2007). This particle also contains some Pb (about 0.94%) (Fig. 7c), which may be attributed to the wearing of axle bearing alloys and wheel balancing devices (Adamiec et al. 2016). Generally, magnetic particles formed from the friction of vehicular parts are rough and angular in surface.

A prismatic-shaped magnetic particle, containing high content of Cr (19.97%), was also observed in the road dusts on the sides of the outer-ring expressway (Fig. 7b). Magnetic particles, with high content of Cr (13%) and irregular in shape, exist in road dust in the urban and industrial areas in Thessaloniki, Greece (Bourliva et al. 2016). Cr in the road dusts mostly comes from the peeling off automobile coatings, wearing of automotive bodies and emissions

**Table 4** Composition of chemical elements in the commercial brake pads (Park et al. 2021) and a rod-like magnetic particle (Fig. 7c) in the road dusts in Baoshan District, Shanghai, Southeast China

| Samples | C (wt%) | O (wt%) | Fe (wt%) | Ca (wt%) | Mg (wt%) | Al (wt%) | Si (wt%) |
|---|---|---|---|---|---|---|---|
| Brake pads | 12.00 ~ 43.60 | 10.20 ~ 27.80 | 5.07 ~ 13.64 | 0.55 ~ 9.20 | 0.63 ~ 2.66 | 0.92 ~ 3.25 | 2.40 ~ 15.80 |
| Magnetic particle | 16.32 | 39.39 | 13.81 | 7.45 | 2.27 | 6.22 | 11.78 |

from stainless steel manufacturers (Bourliva et al. 2016; Wang et al. 2012). According to a test, the content of Cr(VI) in three automotive materials is in a range of 16 and 92 mg $kg^{-1}$ (Wang et al. 2020). Cr content of the road dusts in the traffic area of this study is 315.5 mg $kg^{-1}$ on average. Appreciatively, high content of Cr in the road dusts beside the outer-ring expressway intensively impacted by traffic is attributed to non-exhaust automotive emissions.

Another magnetic particle polymeric in shape in the traffic road dust has high content of Zn, reaching as high as 22.31% (Fig. 7d). ZnO is added to the rubber of tires (Adachi and Tainosho 2004). Zn content in the tire-treading particles attains as high as 9000 mg $kg^{-1}$, in line with the expected value of synthetic rubber, and that in the road dusts usually ranges from 300 to 2600 mg $kg^{-1}$ (Kreider et al. 2010). Zn content in the road dust, where the Zn-rich particle appears, is 377.1 ppm, coinciding with previous studies (Kreider et al. 2010). This suggests that the road dust has ever been added with tire-wearing particles. Zn level in the environment may also be increased by the emissions of automotive exhausts, and antioxidants and dispersants in lubricants (Charlesworth et al. 2011).

### 4.3 Heavy metal accumulation in urban road dusts and its correlations with magnetic signal

Urban soils are often complicated in origin. Besides being inherited from parent rocks, it can also be deeply affected by the filling of guest soils, discharge of solid wastes, and deposition of atmospheric particles. Urban road dusts, on the contrary, solely come from the dry and wet depositions of atmospheric suspended particles and can reflect the presence or content of atmospheric magnetic pollutants more directly.

Compared with urban soils, therefore, urban road dusts are often enriched in more heavy metals. Cu, Zn, Pb, Cd, Cr, Ni, and Mn contents in the road dusts of this study are significantly higher than those in the urban soils in the same areas, as previously reported (Hu et al. 2022). The road dusts in urban areas mainly consist of anthropogenic pollutants, containing high content of toxic heavy metals.

The SPI of heavy metals in the road dusts of the study areas is in the decreasing sequence of Pb > Cd > Zn > Cr > Cu > Mn > Ni > Co (Table 5), of which, Cu, Zn, Pb, Cd, and Cr are > 3, reflecting the degree of heavy pollution.

The road dusts in the different functional areas are different in the SPI. The industrial road dusts are heavily polluted by Zn, Pb, Cd, and Cr, moderately polluted by Cu and Mn, and slightly polluted by Co and Ni. The traffic road dusts are heavily polluted by Cu, Zn, Pb, Cd, and Cr and slightly polluted by Co, Ni, and Mn. The residential road dusts are heavily polluted by Zn, Pb, and Cd, moderately polluted by Cu and Cr, and lightly polluted by Ni and Mn. The agricultural road dusts are heavily polluted by Zn, Pb, Cd, and Cr, moderately polluted by Cu, and lightly polluted by Ni and Mn. Overall, Pb, Cd, Zn, Cr, and Cu are highly accumulated in the road dusts. The PLI analyses also indicate that 30.3% of the road dusts in the study areas are heavily polluted by heavy metals, 44.3% moderately polluted, and 25.4% slightly polluted.

Magnetic particles emitted from industry, traffic, and coal burning usually contain or adsorb toxic heavy metal elements (Ali et al. 2017; Yang et al. 2020). The deposition of magnetic particles, therefore, leads to the enhancement of magnetic strength and heavy metal content in urban topsoils simultaneously (Golden et al. 2017; Oudeika et al. 2020). The enrichment of magnetic particles and heavy metals were observed in the surface soil of an industrial park in Izmit, Turkey, where $\chi_{lf}$ is significantly correlated with the content of Cu, Pb, Cr, and Ni (Canbay et al. 2010). The spatial distribution of $\chi_{lf}$ and heavy metal content in the urban green land in Kaifeng City, China, is

**Table 5** Single-factor Pollution Index (SPI) and Pollution Load Index (PLI) of the road dusts in Baoshan District, Shanghai, Southeast China

| Functional areas | SPI | | | | | | | | PLI |
|---|---|---|---|---|---|---|---|---|---|
| | Cu | Zn | Pb | Cd | Cr | Co | Ni | Mn | |
| Industrial | 2.70 | 6.07 | 4.43 | 4.53 | 3.69 | 1.15 | 1.64 | 2.06 | 2.88 |
| Traffic | 4.86 | 3.59 | 7.40 | 4.98 | 5.20 | 1.35 | 1.40 | 1.49 | 3.14 |
| Residential | 2.41 | 3.14 | 16.81 | 5.68 | 2.24 | 0.71 | 1.14 | 1.13 | 2.49 |
| Agricultural | 2.65 | 3.39 | 6.36 | 4.01 | 3.05 | 0.85 | 1.43 | 1.51 | 2.45 |
| Baoshan District | 3.30 | 4.28 | 8.01 | 4.79 | 3.76 | 1.07 | 1.44 | 1.61 | 2.90 |

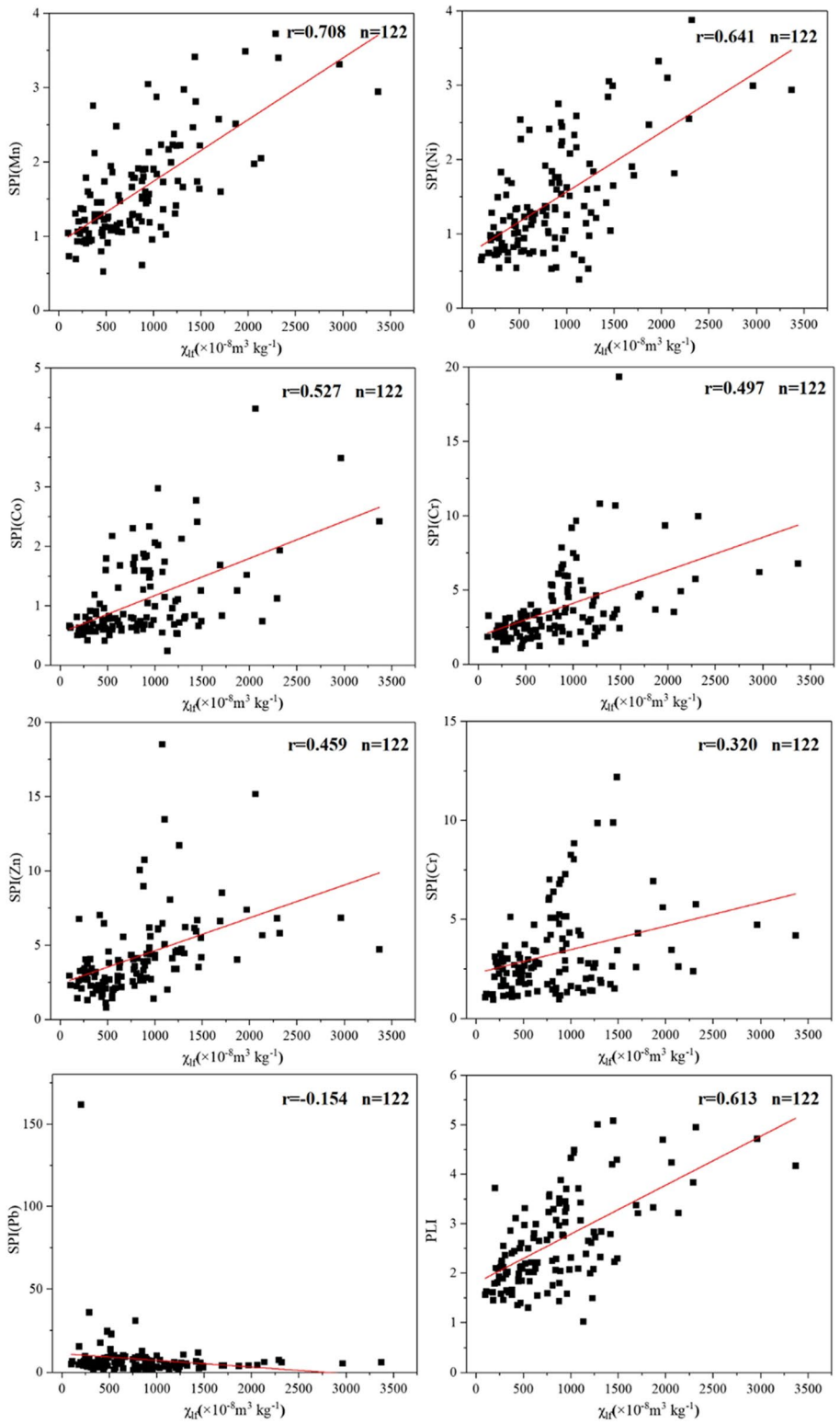


**Fig. 8** Correlations between magnetic susceptibility ($\chi_{lf}$) and Single-factor Pollution Index (SPI), and Pollution Load Index (PLI) in the road dusts in Baoshan District, Shanghai, Southeast China

closely related to the intensity of anthropogenic impacts, where $\chi_{lf}$ is significantly correlated with the content of Cu, Zn, Pb, Cd, Cr, and Ni (Liu et al. 2016). $\chi_{lf}$ of the urban topsoils in Baotou City, southern Mongolia Plateau, China, is significantly correlated with the content of Zn, Pb, Cr, Mn, and Fe (Wang et al. 2018). The urban soils highly impacted by industrial activities in Baoshan District, Shanghai, were investigated 10 years ago, in which, $\chi_{lf}$ is positively significantly correlated with the content of Pb, Cd, Ni, and Mn ($r$=0.781, 0.473, 0.365, and 0.835, respectively; $n$=27; $p$<0.01), and also significantly correlated with Cu, Zn, and Cr ($r$=0.227, 0.214, and 0.218, respectively; $n$=27; $p$<0.05) (Hu et al. 2007). In recent years, the same areas in Baoshan District were investigated again, where more significant correlations between $\chi_{lf}$ and content of Cu, Zn, Pb, Cd, Cr, Ni, Mn, and Fe were observed ($r$=0.726, 0.873, 0.873, 0.726, 0.873, 0.873, 0.726, 0.873, 0.726, 0.873, and 0.654 respectively; $p$<0.01) (Hu et al. 2022). This suggests the continuous deposition of metal-containing magnetic particles in the industrial/urban areas.

$\chi_{lf}$ of road dusts near the largest copper smelter in Southeast Europe is $325.65\times10^{-8}$ $m^3$ $kg^{-1}$, which is significantly positively correlated with the content of Cu, Zn, Pb, Cd, and Ni and also strongly correlated with the (PLI) (Jordanova et al. 2021). That of street dusts in Warsaw, Poland, ranging from 470 to $1025\times10^{-8}$ $m^3$ $kg^{-1}$, is significantly positively correlated with the content of Zn, Cd, Co, Ni, and Mn, where the content of anthropogenic magnetic particles is closely related to the flux of vehicles (Dytłow et al. 2019). That of road dusts in Lanzhou, China, $449.88\times10^{-8}$ $m^3$ $kg^{-1}$ on average, is positively significantly correlated with the content of Cu, Zn, Pb, Ni, and Mn (Wang et al. 2012).

In this study, $\chi_{lf}$ of all the road dusts of the study areas is positively significantly correlated with the content of Cu, Zn, Cr, Co, Ni, Mn, and Fe ($r$=0.320, 0.459, 0.497, 0.527, 0.641, 0.708, and 0.871, $n$=122; $p$<0.01), and is also positively correlated with PLI value ($r$=0.613, $p$<0.01) (Fig. 8), further proving that the magnetic signal of urban road dusts can indicate heavy metal pollution.

$\chi_{lf}$ of the industrial, traffic, residential, and agricultural road dusts is all significantly correlated with their PLI values ($r$=0.758, 0.827, 0.506, and 0.741, respectively; $p$<0.01 or 0.05). However, the correlations between $\chi_{lf}$ and heavy metal content of the road dusts in the four areas are often different. $\chi_{lf}$ of the industrial road dusts is positively significantly correlated with the content of Cu, Pb, Cd, Cr, Co, Ni, Mn, and Fe ($p$<0.01); that of the traffic road dusts is positively significantly with Cu, Zn, Cd, Cr, Co, Ni, Mn, and Fe ($p$<0.01); that of the residential road dusts is only positively significantly with Cu, Cr, and Fe ($p$<0.01) and Ni ($p$<0.05); and that of the agricultural road dusts is positively significantly with Cd, Cr, Co, Ni, and Fe ($p$<0.01) (Table 6).

Generally, the industrial and traffic road dusts, highly impacted by industrial and vehicular emissions, and more enriched in anthropogenic magnetic particles, have more significant correlations between $\chi_{lf}$ and heavy metal content. For example, the industrial road dusts located near the Baosteel Machinery Factory at Site No. 36 reach as high as $3367.3\times10^{-8}$ $m^3$ $kg^{-1}$ in $\chi_{lf}$, correlated with high content of Zn (1308.8 mg $kg^{-1}$), Cr (431.8 mg $kg^{-1}$), Mn (2090.1 mg $kg^{-1}$), and Fe (127.1 g $kg^{-1}$). The traffic road dusts beside the outer-ring expressway at Site No.12 is $1482.0\times10^{-8}$ $m^3$ $kg^{-1}$in $\chi_{lf}$, correlated with high content of Cu (349.4 mg $kg^{-1}$), Zn (475.7 mg $kg^{-1}$), Cr (1453.1 mg $kg^{-1}$), Co (16.0 mg $kg^{-1}$), Ni (95.7 mg $kg^{-1}$), Mn (920.0 mg $kg^{-1}$), and Fe (84.4 g $kg^{-1}$).

For comparison, the agricultural and residential road dusts are lower in $\chi_{lf}$ and have weak correlations between $\chi_{lf}$ and heavy metal content, as they are relatively far away from industrial parks and transportation hubs, and contain lower content of anthropogenic magnetic particles.

### 4.4 Principal component analyses (PCA)

$X_{lf}$ value and content of heavy metals (Cu, Zn, Pb, Cd, Cr, Co, Ni, Mn, and Fe) in the 122 road dust samples of the study areas are further analyzed using the PCA method (Fig. 9). The results indicated that the three components contribute to 72.033% of the total variance (Table 7).

**Table 6** Correlation between magnetic susceptibility ($\chi_{lf}$) and heavy metal content of the road dusts in different functional areas in Baoshan District, Shanghai, Southeast China

| | Functional areas | Cu | Zn | Pb | Cd | Cr | Co | Ni | Mn | Fe |
|---|---|---|---|---|---|---|---|---|---|---|
| $\chi_{lf}$ | Industrial | 0.580** | 0.165 | 0.491** | 0.577** | 0.702** | 0.623** | 0.707** | 0.684** | 0.744** |
| | Traffic | 0.917** | 0.614** | -0.322 | 0.547** | 0.876** | 0.491** | 0.795** | 0.574** | 0.813** |
| | Residential | 0.665** | 0.179 | -0.122 | 0.224 | 0.462** | 0.437 | 0.589* | 0.341 | 0.776** |
| | Agricultural | 0.169 | 0.418 | 0.095 | 0.626** | 0.749** | 0.671** | 0.758** | 0.329 | 0.869** |
| | Baoshan District | 0.320** | 0.459** | -0.154* | 0.171 | 0.497** | 0.527** | 0.641** | 0.708** | 0.871** |

*Indicates the significant level ( $p$<0.05)

**Indicates the extremely significant level ($p$<0.01)

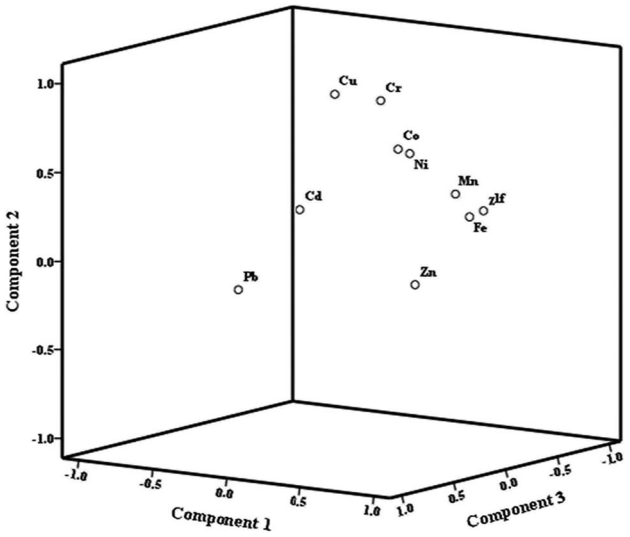


**Fig. 9** Rotational spatial distribution of magnetic susceptibility ($\chi_{lf}$) and heavy metal contents in the road dusts in Baoshan District, Shanghai, Southeast China

Principal component 1 (PC1) explains 46.671% of the total variance, with an initial eigenvalue of 4.667. $\chi_{lf}$, Zn, Mn, and Fe show high positive loads in the PC1. Moreover, they are positively significantly correlated with each other ($p < 0.01$) (Table 8), implying their similar provenance. Fe-containing particles are highly emitted from burning cylinders and frictions of brakes (Dytłow et al. 2019). Zn mostly comes from the wearing of treading tires and corrosion of galvanized automobile parts (Iijima et al. 2007; Lu et al. 2017), and Mn tightly combined with Fe is emitted from industrial smelting and coal combustion (Men et al. 2018). Appreciatively, the PC1 is mainly contributed by Fe-containing magnetic particles in the road dusts emitted from vehicles and industrial smelting.

**Table 7** Principal component analyses (PCA) on magnetic susceptibility ($\chi_{lf}$) and heavy metal contents in the road dusts in Baoshan District, Shanghai, Southeast China

| Elements | Component 1 | Component 2 | Component 3 |
|---|---|---|---|
| $\chi_{lf}$ | 0.880 | 0.308 | −0.119 |
| Cu | 0.228 | 0.871 | −0.058 |
| Zn | 0.688 | −0.069 | 0.268 |
| Pb | −0.122 | −0.098 | 0.826 |
| Cd | 0.198 | 0.361 | 0.681 |
| Cr | 0.228 | 0.871 | −0.058 |
| Co | 0.427 | 0.635 | 0.058 |
| Ni | 0.555 | 0.633 | 0.129 |
| Mn | 0.722 | 0.393 | −0.074 |
| Fe | 0.823 | 0.277 | −0.065 |
| Total eigenvalues | 4.667 | 1.384 | 1.153 |
| Percentage of total variance | 46.671 | 13.836 | 11.526 |
| Cumulative variance (%) | 46.671 | 60.057 | 72.033 |

Principal component 2 (PC2) explains 13.836% of the total variance, in which, Cu, Cr, Co, and Ni show high positive loads. Likewise, the four are positively significantly correlated with each other ($p < 0.01$) (Table 8). Cu and Cr in the road dusts may come from the fractions of automobile brakes (Hassan 2012; Thorpe and Harrison 2008). Cr may also come from the wearing of Cr coatings in vehicular body or exhausts from metallurgy and tanning. Co may stem from the industrial production of magnets, catalysts, alloys, and vehicular batteries (Hao et al. 2017; Sun et al. 2019). Ni may come from fossil fuel combustion and metal smelting (Duong and Lee 2009; Manno et al. 2006). In short, the PC2 is also contributed by the emissions from industry and traffic but is more complicated in sources.

Principal component 3 (PC3) explains 11.526% of the total variance and shows significant loads for Pb and Cd (Table 8). Pb content is only positively significantly correlated with Cd content ($p < 0.01$), and not significantly with $\chi_{lf}$ and the other heavy metals ($p > 0.05$) (Table 8). This suggests that Pb is different in source from magnetic particles and its bearing heavy metals. The high content of Pb but low $\chi_{lf}$ in the road dusts besides a residential site at Dachang Town of the district suggest the invasion of non-magnetic Pb pollutants such as lead-rich paint, batteries, furniture parts, and other domestic garbage. This coincides with an extremely high Pb content but non-high $\chi_{lf}$ in a residential topsoil of the same areas, as previously reported (Hu et al. 2022). Cd is not significantly correlated with $\chi_{lf}$ either. Cd may exist in non-magnetic industrial or building dusts (Schwab et al. 2014; Wang et al. 2022, 2016). In short, the PC3 in the road dusts may reflect non-magnetic heavy metal sources.

### 4.5 Using $\chi_{lf}$ of urban road dust for monitoring urban environment

Solidified roads in Shanghai are mostly cleaned twice a week. The constituents of road dust, therefore, almost solely stem from the dry and wet atmospheric deposition. In this study, $\chi_{lf}$ of the road dusts in the four areas is almost linearly correlated with Fe content ($n = 122$, $r = 0.871$; $p < 0.001$), fully suggesting that the magnetism of road dust is completely contributed by Fe-bearing particles, combined with toxic heavy metals. Such fine metal-bearing particles are suspended in the urban atmosphere, which pose threat to human health. Compared with routine chemical analyses, the magnetic measurements of samples are simple, rapid, and low-cost. Through monitoring magnetic signal of road dusts, we can quickly know the concentration of suspended

**Table 8** Correlation analyses between the two of magnetic susceptibility ($\chi_{lf}$) and heavy metal content of the road dusts in the different functional areas in Baoshan District, Shanghai, Southeast China

| | $\chi_{lf}$ | Cu | Zn | Pb | Cd | Cr | Co | Ni | Mn | Fe |
|---|---|---|---|---|---|---|---|---|---|---|
| $\chi_{lf}$ | 1 | | | | | | | | | |
| Cu | 0.320** | 1 | | | | | | | | |
| Zn | 0.459** | 0.137 | 1 | | | | | | | |
| Pb | −0.154 | 0.014 | 0.019 | 1 | | | | | | |
| Cd | 0.171 | 0.369** | 0.206* | 0.238** | 1 | | | | | |
| Cr | 0.497** | 0.801** | 0.149 | −0.082 | 0.238** | 1 | | | | |
| Co | 0.527** | 0.557** | 0.322** | −0.079 | 0.301** | 0.518** | 1 | | | |
| Ni | 0.641** | 0.554** | 0.329** | −0.046 | 0.421** | 0.615** | 0.600** | 1 | | |
| Mn | 0.708** | 0.342** | 0.303** | −0.124 | 0.243** | 0.455** | 0.569** | 0.613** | 1 | |
| Fe | 0.871** | 0.297** | 0.360** | −0.111 | 0.253** | 0.487** | 0.370** | 0.569** | 0.647** | 1 |

*Indicates the extremely significant level $p < 0.05$

**Indicates the extremely significant level $p < 0.01$

metal-bearing particles in the urban atmosphere and further track the sources of emissions. The deposition of natural dust can be predicted from climatic data after the establishment of models (Bagheri-Bodaghabadi and Jafari 2022). Magnetic parameters of road dust may also contribute to predict the fluxes of anthropogenic emissions in the urban areas. It should be further studied however.

## 5 Conclusions

The road dusts in Baoshan District of Shanghai are alkaline, of which, $\chi_{lf}$ is $838.7 \times 10^{-8}$ $m^3$ $kg^{-1}$ on average, about 30 times the magnetic background of the soils in Shanghai. $\chi_{lf}$ of the industrial and traffic road dusts is significantly higher than that of the others, suggesting the significant influences of industrial and traffic emissions on urban ground. $\chi_{fd}$% of all the road dusts is less than 4% and that of 89.3% is less than 2%, indicating the accumulation of anthropogenic coarse magnetic particles.

Magnetic spherules, mainly composed of Fe oxides, commonly exist in the road dusts of Baoshan District, which are more in content and coarser in grain size in the industrial and traffic areas, implying that they mostly come from industrial and vehicular emissions. Flake-shaped, rod-like, and other irregular magnetic particles were also observed in the road dusts, which may originate from metal processing and wearing of vehicular brake pads, tires, and other body materials.

The SPI analyses indicate that the road dusts in Baoshan District are heavily polluted by Cu, Zn, Pb, Cd, and Cr. $\chi_{lf}$ of the road dusts is significantly correlated with the contents of Cu, Zn, Cr, Co, Ni, Mn, and Fe ($p < 0.01$). Moreover, $\chi_{lf}$ of the road dusts is significantly positively correlated with PLI value ($p < 0.01$), suggesting that $\chi_{lf}$ can indicate the accumulation of heavy metals in the road dusts effectively. The PCA also illustrates the presence of artificial Fe-bearing magnetic particles combined with toxic heavy metals in the road dusts.

**Funding** This work was supported by the National Natural Science Foundation of China (Nos. 42371056 and 41877005).

## Declarations

**Competing interest** The authors declare no competing interests.

## References

Abbasi S, Keshavarzi B, Moore F, Hopke PK, Kelly FJ, Dominguez AO (2020) Elemental and magnetic analyses, source identification, and oxidative potential of airborne, passive, and street dust particles in Asaluyeh County. Iran Sci Total Environ 707:136132. https://doi.org/10.1016/j.scitotenv.2019.136132

Adachi K, Tainosho Y (2004) Characterization of heavy metal particles embedded in tire dust. Environ Int 30(8):1009–1017. https://doi.org/10.1016/j.envint.2004.04.004

Adamiec E, Jarosz-Krzeminska E, Wieszala R (2016) Heavy metals from non-exhaust vehicle emissions in urban and motorway road dusts. Environ Monit Assess 188(6):369. https://doi.org/10.1007/s10661-016-5377-1

Aguilar Y, Bautista F, Quintana P, Aguilar D, Trejo-Tzab R, Goguitchaichvili A, Chan-Te R (2021) Color as a new proxy technique for the identification of road dust samples contaminated with potentially toxic elements: the case of Mérida, Yucatán, México. Atm 12(4):483. https://doi.org/10.3390/atmos12040483

Ali MU, Liu G, Yousaf B, Abbas Q, Ullah H, Munir MAM, Fu B (2017) Pollution characteristics and human health risks of potentially (eco)toxic elements (PTEs) in road dust from metropolitan area of Hefei, China. Chemosphere 181:111–121. https://doi.org/10.1016/j.chemosphere.2017.04.061

Bagheri-Bodaghabadi M, Jafari M (2022) The dust deposition model (DDM): An empirical model for monitoring dust deposition using meteorological data over the Isfahan province in central Iran. Catena. https://doi.org/10.1016/j.catena.2021.105952

Blaha U, Appel E, Stanjek H (2008) Determination of anthropogenic boundary depth in industrially polluted soil and semi-quantification of heavy metal loads using magnetic susceptibility. Environ Pollut 156(2):278–289. https://doi.org/10.1016/j.envpol.2008.02.013

Bourliva A, Papadopoulou L, Aidona E (2016) Study of road dust magnetic phases as the main carrier of potentially harmful trace elements. Sci Total Environ 553:380–391. https://doi.org/10.1016/j.scitotenv.2016.02.149

Bourliva A, Kantiranis N, Papadopoulou L, Aidona E, Christophoridis C, Kollias P, Fytianos K (2018) Seasonal and spatial variations of magnetic susceptibility and potentially toxic elements (PTEs) in road dusts of Thessaloniki city, Greece: a one-year monitoring period. Sci Total Environ 639:417–427. https://doi.org/10.1016/j.scitotenv.2018.05.170

Bucko MS, Magiera T, Johanson B, Petrovsky E, Pesonen LJ (2011) Identification of magnetic particulates in road dust accumulated on roadside snow using magnetic, geochemical and micro-morphological analyses. Environ Pollut 159(5):1266–1276. https://doi.org/10.1016/j.envpol.2011.01.030

Canbay M, Aydin A, Kurtulus C (2010) Magnetic susceptibility and heavy-metal contamination in topsoils along the Izmit Gulf coastal area and IZAYTAS (Turkey). J Appl Geophys 70(1):46–57. https://doi.org/10.1016/j.jappgeo.2009.11.002

Cao L, Appel E, Hu S, Yin G, Lin H, Rösler W (2015) Magnetic response to air pollution recorded by soil and dust-loaded leaves in a changing industrial environment. Atmos Environ 119:304–313. https://doi.org/10.1016/j.atmosenv.2015.06.017

Charlesworth S, De Miguel E, Ordonez A (2011) A review of the distribution of particulate trace elements in urban terrestrial environments and its application to considerations of risk. Environ Geochem Health 33(2):103–123. https://doi.org/10.1007/s10653-010-9325-7

Dearing JA, Dann RJL, Hay K, Lees JA, Loveland PJ, Maher BA, O'Grady K (1996) Frequency-dependent susceptibility measurements of environmental materials. Geophys J Int 124(1):228–240. https://doi.org/10.1111/j.1365-246x.1996.tb06366.x

Duong TTT, Lee B-K (2009) Partitioning and mobility behavior of metals in road dusts from national-scale industrial areas in Korea. Atmos Environ 43(22–23):3502–3509. https://doi.org/10.1016/j.atmosenv.2009.04.036

Dytłow S, Winkler A, Górka-Kostrubiec B, Sagnotti L (2019) Magnetic, geochemical and granulometric properties of street dust from Warsaw (Poland). J Appl Geophys 169:58–73. https://doi.org/10.1016/j.jappgeo.2019.06.016

Fabijańczyk P, Zawadzki J, Magiera T, Szuszkiewicz M (2016) A methodology of integration of magnetometric and geochemical soil contamination measurements. Geoderma 277:51–60. https://doi.org/10.1016/j.geoderma.2016.05.009

Golden N, Zhang C, Potito AP, Gibson PJ, Bargary N, Morrison L (2017) Impact of grass cover on the magnetic susceptibility measurements for assessing metal contamination in urban topsoil. Environ Res 155:294–306. https://doi.org/10.1016/j.envres.2017.02.032

Górka-Kostrubiec B, Świetlik R, Szumiata T, Dytłow S, Trojanowska M (2023) Integration of chemical fractionation, Mössbauer spectrometry, and magnetic methods for identification of Fe phases bonding heavy metals in street dust. J Environ Sci 124:875–891. https://doi.org/10.1016/j.jes.2022.02.015

Gunawardana C, Goonetilleke A, Egodawatta P, Dawes L, Kokot S (2012) Source characterisation of road dust based on chemical and mineralogical composition. Chemosphere 87(2):163–170. https://doi.org/10.1016/j.chemosphere.2011.12.012

Hao H, Cheng X, Liu Z, Zhao F (2017) China's traction battery technology roadmap: Targets, impacts and concerns. Energy Policy 108:355–358. https://doi.org/10.1016/j.enpol.2017.06.011

Hassan SKM (2012) Metal concentrations and distribution in the household, stairs and entryway dust of some Egyptian homes. Atmos Environ 54:207–215. https://doi.org/10.1016/j.atmosenv.2012.02.013

Hu XF, Su Y, Ye R, Li XQ, Zhang GL (2007) Magnetic properties of the urban soils in Shanghai and their environmental implications. Catena 70(3):428–436. https://doi.org/10.1016/j.catena.2006.11.010

Hu XF, Li M, He ZC, Cui L, Liu R, Wang XD, Wang ZH (2022) Magnetic responses to heavy metal pollution of the industrial soils in Shanghai: implying the influences of anthropogenic magnetic dustfall on urban environment. J Appl Geophys. https://doi.org/10.1016/j.jappgeo.2022.104544

Iijima A, Sato K, Yano K, Tago H, Kato M, Kimura H, Furuta N (2007) Particle size and composition distribution analysis of automotive brake abrasion dusts for the evaluation of antimony sources of airborne particulate matter. Atmos Environ 41(23):4908–4919. https://doi.org/10.1016/j.atmosenv.2007.02.005

Jordanova D, Goddu SR, Kotsev T, Jordanova N (2013) Industrial contamination of alluvial soils near Fe–Pb mining site revealed by magnetic and geochemical studies. Geoderma 192:237–248. https://doi.org/10.1016/j.geoderma.2012.07.004

Jordanova D, Jordanova N, Petrov P (2014) Magnetic susceptibility of road deposited sediments at a national scale–relation to population size and urban pollution. Environ Pollut 189:239–251. https://doi.org/10.1016/j.envpol.2014.02.030

Jordanova N, Jordanova D, Tcherkezova E, Georgieva B, Ishlyamski D (2021) Advanced mineral magnetic and geochemical investigations of road dusts for assessment of pollution in urban areas near the largest copper smelter in SE Europe. Sci Total Environ 792:148402. https://doi.org/10.1016/j.scitotenv.2021.148402

Jose J, Srimuruganandam B (2021) Application of micro-morphology in the physical characterization of urban road dust. Particuology 54:146–155. https://doi.org/10.1016/j.partic.2020.05.002

Kacer J, Altmaier R, Latta D, O'Shaughnessy PT, Cwiertny DM (2023) Evaluation of airborne particulates and associated metals originating from steel slag applied to rural unpaved roads. Environ Sci Atmos 3(1):238–246. https://doi.org/10.1039/d2ea00040g

Karimi R, Ayoubi S, Jalalian A, Sheikh-Hosseini AR, Afyuni M (2011) Relationships between magnetic susceptibility and heavy metals in urban topsoils in the arid region of Isfahan, central Iran. J Appl Geophys 74(1):1–7. https://doi.org/10.1016/j.jappgeo.2011.02.009

Kim W, Doh S-J, Park Y-H, Yun S-T (2007) Two-year magnetic monitoring in conjunction with geochemical and electron microscopic data of roadside dust in Seoul. Korea Atmospheric Environment 41(35):7627–7641. https://doi.org/10.1016/j.atmosenv.2007.05.050

Kreider ML, Panko JM, McAtee BL, Sweet LI, Finley BL (2010) Physical and chemical characterization of tire-related particles: comparison of particles generated using different methodologies. Sci Total Environ 408(3):652–659. https://doi.org/10.1016/j.scitotenv.2009.10.016

Li X, Feng L (2010) Spatial distribution of hazardous elements in urban topsoils surrounding Xi'an industrial areas, (NW, China): controlling factors and contamination assessments. J Hazard Mater 174(1–3):662–669. https://doi.org/10.1016/j.jhazmat.2009.09.102

Liu E, Yan T, Birch G, Zhu Y (2014) Pollution and health risk of potentially toxic metals in urban road dust in Nanjing, a mega-city of China. Sci Total Environ 476–477:522–531. https://doi.org/10.1016/j.scitotenv.2014.01.055

Liu D, Ma J, Sun Y, Li Y (2016) Spatial distribution of soil magnetic susceptibility and correlation with heavy metal pollution in Kaifeng City, China. Catena 139:53–60. https://doi.org/10.1016/j.catena.2015.11.004

Logiewa A, Miazgowicz A, Krennhuber K, Lanzerstorfer C (2020) Variation in the concentration of metals in road dust size fractions between 2 microm and 2 mm: results from three metallurgical centres in Poland. Arch Environ Contam Toxicol 78(1):46–59. https://doi.org/10.1007/s00244-019-00686-x

Lu SG, Yu XL, Chen YY (2016) Magnetic properties, microstructure and mineralogical phases of technogenic magnetic particles (TMPs) in urban soils: Their source identification and environmental implications. Sci Total Environ 543(Pt A):239–247. https://doi.org/10.1016/j.scitotenv.2015.11.046

Lu X, Pan H, Wang Y (2017) Pollution evaluation and source analysis of heavy metal in roadway dust from a resource-typed industrial city in Northwest China. Atmos Pollut Res 8(3):587–595. https://doi.org/10.1016/j.apr.2016.12.019

Magiera T, Jabłońska M, Strzyszcz Z, Rachwal M (2011) Morphological and mineralogical forms of technogenic magnetic particles in industrial dusts. Atmos Environ 45(25):4281–4290. https://doi.org/10.1016/j.atmosenv.2011.04.076

Magiera T, Zawadzki J, Szuszkiewicz M, Fabijanczyk P, Steinnes E, Fabian K, Miszczak E (2018) Impact of an iron mine and a nickel smelter at the Norwegian/Russian border close to the Barents Sea on surface soil magnetic susceptibility and content of potentially toxic elements. Chemosphere 195:48–62. https://doi.org/10.1016/j.chemosphere.2017.12.060

Magiera T, Gorka-Kostrubiec B, Szumiata T, Wawer M (2021) Technogenic magnetic particles from steel metallurgy and iron mining in topsoil: indicative characteristic by magnetic parameters and Mossbauer spectra. Sci Total Environ 775:145605. https://doi.org/10.1016/j.scitotenv.2021.145605

Manno E, Varrica D, Dongarrà G (2006) Metal distribution in road dust samples collected in an urban area close to a petrochemical plant at Gela. Sicily Atmos Environ 40(30):5929–5941. https://doi.org/10.1016/j.atmosenv.2006.05.020

Men C, Liu R, Wang Q, Guo L, Shen Z (2018) The impact of seasonal varied human activity on characteristics and sources of heavy metals in metropolitan road dusts. Sci Total Environ 637–638:844–854. https://doi.org/10.1016/j.scitotenv.2018.05.059

Oudeika MS, Altinoglu FF, Akbay F, Aydin A (2020) The use of magnetic susceptibility and chemical analysis data for characterizing heavy metal contamination of topsoil in Denizli city Turkey. J Appl Geophys. https://doi.org/10.1016/j.jappgeo.2020.104208

Panko JM, Chu J, Kreider ML, Unice KM (2013) Measurement of airborne concentrations of tire and road wear particles in urban and rural areas of France, Japan, and the United States. Atmos Environ 72:192–199. https://doi.org/10.1016/j.atmosenv.2013.01.040

Pant P, Harrison RM (2013) Estimation of the contribution of road traffic emissions to particulate matter concentrations from field measurements: a review. Atmos Environ 77:78–97. https://doi.org/10.1016/j.atmosenv.2013.04.028

Park J, Joo B, Seo H, Song W, Lee JJ, Lee WK, Jang H (2021) Analysis of wear induced particle emissions from brake pads during the worldwide harmonized light vehicles test procedure (WLTP). Wear 466:203539. https://doi.org/10.1016/j.wear.2020.203539

Petrovský E, Zbořil R, Grygar TM, Kotlík B, Novák J, Kapička A, Grison H (2013) Magnetic particles in atmospheric particulate matter collected at sites with different level of air pollution. Stud Geophys Geod 57(4):755–770. https://doi.org/10.1007/s11200-013-0814-x

Rao Z, Guo W, Xie L, Huang C, Liu X, Hua H, Chen F (2015) High resolution δ13CTOC and magnetic susceptibility data from the late Early Pleistocene southern margins of the Chinese Loess Plateau. Org Geochem 87:78–85. https://doi.org/10.1016/j.orggeochem.2015.08.004

Schwab O, Bayer P, Juraske R, Verones F, Hellweg S (2014) Beyond the material grave: life cycle impact assessment of leaching from secondary materials in road and earth constructions. Waste Manag 34(10):1884–1896. https://doi.org/10.1016/j.wasman.2014.04.022

Shilton VF, Booth CA, Smith JP, Giess P, Mitchell DJ, Williams CD (2005) Magnetic properties of urban street dust and their relationship with organic matter content in the West Midlands. UK Atmos Environ 39(20):3651–3659. https://doi.org/10.1016/j.atmosenv.2005.03.005

Strzałkowska E (2022) Rare earth elements and other critical elements in the magnetic fraction of fly ash from several Polish power plants. Int J Coal Geol. https://doi.org/10.1016/j.coal.2022.104015

Sun X, Hao H, Liu Z, Zhao F, Song J (2019) Tracing global cobalt flow: 1995–2015. Resour Conserv Recycl 149:45–55. https://doi.org/10.1016/j.resconrec.2019.05.009

Sun DH, Su RX, Chen FH, Yuan BY, David R (2001) Composition susceptibility and input flux of present aeolian dust over loess plateau of China. Acta Geographica Sinica 56(2):171–180. https://doi.org/10.11821/dlxb2019110021

Thorpe A, Harrison RM (2008) Sources and properties of non-exhaust particulate matter from road traffic: a review. Sci Total Environ 400(1–3):270–282. https://doi.org/10.1016/j.scitotenv.2008.06.007

Tomlinson DL, Wilson JG, Harris CR, Jeffrey DW (1980) Problems in the assessment of heavy-metal levels in estuaries and the formation of a pollution index. Helgolander Meeresunters 33:566–575. https://doi.org/10.1007/BF02414780

USDA (United States Department of Agriculture), NRCS (Natural Resources Conservation Service) (2004) Soil Survey Laboratory Manual. Soil Survey Investigations Report No. 42, Version 4.0, pp 173–204

Wang Y, Zhang Y, Schauer JJ, de Foy B, Guo B, Zhang Y (2016) Relative impact of emissions controls and meteorology on air pollution mitigation associated with the Asia-Pacific Economic Cooperation (APEC) conference in Beijing, China. Sci Total Environ 571:1467–1476. https://doi.org/10.1016/j.scitotenv.2016.06.215

Wang B, Xia D, Yu Y, Chen H, Jia J (2018) Source apportionment of soil-contamination in Baotou City (North China) based on a combined magnetic and geochemical approach. Sci Total Environ 642:95–104. https://doi.org/10.1016/j.scitotenv.2018.06.050

Wang G, Chen J, Zhang W, Ren F, Chen Y, Fang A, Ma L (2019) Magnetic properties of street dust in Shanghai, China and its relationship to anthropogenic activities. Environ Pollut 255(Pt 1):113214. https://doi.org/10.1016/j.envpol.2019.113214

Wang S, Wang L, Huan Y, Wang R, Liang T (2022) Concentrations, spatial distribution, sources and environmental health risks of potentially toxic elements in urban road dust across China. Sci Total Environ 805:150266. https://doi.org/10.1016/j.scitotenv.2021.150266

Wang Y, Wang YG, Luo HL (1992) Soil environmental background values in Shanghai (in Chinese). China Environmental Science Press, Beijing, pp 55–77

Wang G, Oldfield F, Xia D, Chen F, Liu X, Zhang W (2012) Magnetic properties and correlation with heavy metals in urban street dust: a case study from the city of Lanzhou, China. Atmosph Environ. https://doi.org/10.1016/j.atmosenv.2011.09.059

Wang G, Ren F, Chen J, Liu Y, Ye F, Oldfield F, . . . Zhang X (2017) Magnetic evidence of anthropogenic dust deposition in urban soils of Shanghai, China. Geochem 77(3):421–428. https://doi.org/10.1016/j.chemer.2017.07.007

Wang K, Fu JY, Guo JY, Ying YJ (2020) Research on determination method for hexavalent chromium in automotive materials (in Chinese). Automob Parts (02):78–80. https://doi.org/10.19466/j.cnki.1674-1986.2020.02.018

Wei B, Yang L (2010) A review of heavy metal contaminations in urban soils, urban road dusts and agricultural soils from China. Microchem J 94(2):99–107. https://doi.org/10.1016/j.microc.2009.09.014

Xia D, Wang B, Yu Y, Jia J, Nie Y, Wang X, Xu S (2014) Combination of magnetic parameters and heavy metals to discriminate soil-contamination sources in Yinchuan–a typical oasis city of Northwestern China. Sci Total Environ 485–486:83–92. https://doi.org/10.1016/j.scitotenv.2014.03.070

Yang T, Liu Q, Chan L, Cao G (2007) Magnetic investigation of heavy metals contamination in urban topsoils around the East Lake, Wuhan. China Geophys J Int 171(2):603–612. https://doi.org/10.1111/j.1365-246X.2007.03558.x

Yang T, Liu Q, Li H, Zeng Q, Chan L (2010) Anthropogenic magnetic particles and heavy metals in the road dust: magnetic identification and its implications. Atmos Environ 44(9):1175–1185. https://doi.org/10.1016/j.atmosenv.2009.12.028

Yang P, Drohan PJ, Yang M (2020) Patterns in soil contamination across an abandoned steel and iron plant: Proximity to source and seasonal wind direction as drivers. Catena. https://doi.org/10.1016/j.catena.2020.104537

Ye R, Hu XF, Pan Y, Su Y, ZHANG, G. L. (2007) Spatial distribution of heavy metals in urban topsoil in Baoshan District, Shanghai (in Chinese). Soils 39:393–399

Zhang GL, Gong ZT (2012) Soil Survey Laboratory Methods (in Chinese). Sci Press, Beijing, pp 119–183